Available online at www.sciencedirect.com
SCIENCE DIRECT®
Thermochimica Acta 424 (2004) 183–199
thermochimica acta
www.elsevier.com/locate/tca

Application of the third-law methodology to investigation of decomposition kinetics

Boris V. L'vov*

Department of Analytical Chemistry, St. Petersburg State Polytechnic University, St. Petersburg 195251, Russia

Received 3 February 2004; received in revised form 28 April 2004; accepted 10 May 2004
Available online 13 July 2004

Abstract

The most important results obtained since the first application (in 2002) of the third-law methodology to kinetic studies of decomposition reactions are considered. The third-law method has been significantly improved and extended to powdered and melted materials. The use of the average values of molar entropy greatly simplified its application to materials with unknown product composition and/or unknown thermodynamic parameters. The order of magnitude higher precision and low susceptibility of the third-law method to the self-cooling compared with the Arrhenius-plots method, guarantees measurement of the E parameter with the error less than 2%. A significant reduction of experimental time and a possibility of simple evaluation of self-cooling are the additional advantages of this method.

The application of the third-law method to decomposition studies permitted to support the basic assumptions underlying the physical approach to interpretation of decomposition kinetics. A good fit of experiment to theory for the ratio of the initial decomposition temperature to the E parameter, the peculiarities of carbonate decomposition in CO_2 and regularities of solid and melted nitrate decomposition are in complete agreement with the mechanism of dissociative evaporation and consumption of a part τ of the condensation energy by reactant. It has become possible to evaluate the τ parameter a priori on the basis of thermodynamic features of the low-volatility product. From comparison of the E parameters with the molar enthalpies of the implied reactions, the decomposition mechanisms of 40 different reactants are identified. Some peculiarities in evolution of gaseous products in atomic and molecular forms are interpreted in accordance with the crystal symmetry of reactants. The earlier theoretical evaluations of the self-cooling effect, which can reach in high vacuum several ten degrees, are supported experimentally.

Keywords: Decomposition mechanisms for 40 reactants; Peculiarities of carbonate decomposition in CO_2; Physical approach; Retardation effect of melting; Self-cooling effect; Third-law method

1. Introduction

Not great length of time has yet elapsed since the appearance (in July 2002) of the first paper on application of the third-law method to investigation of decomposition kinetics [1]. Nevertheless, because of the importance of findings over this brief period for theory and methodology, there is a need for consistent presentation of results reported up to now only partly in rather scattered publications [2–12]. The first part of this review will contain a short description of the physical approach to decomposition kinetics (PA-theory) that provides the basis for other studies. The second part of paper will present the third-law methodology with all operational (procedure) details including some recent improvements and, also, discussion of advantages of this method in comparison with the traditional Arrhenius-plots and second-law methods. The third part of this paper will be devoted to consideration of the main results obtained with the use of this methodology. Some of them are concerned with the proof and development of PA-theory and some, what is the most important, with the analysis of decomposition mechanisms and regularities revealed for several classes of inorganic reactants (oxides, nitrides, hydroxides, carbonates, sulfates, nitrates and hydrates).

* Tel.: +7-812-552-7741; fax: +7-812-247-4384.
E-mail address: borislvov@rambler.ru (B.V. L'vov).

0040-6031/$ – see front matter © 2004 Elsevier B.V. All rights reserved.
doi:10.1016/j.tca.2004.05.012

2. Physical approach to decomposition kinetics

2.1. The basic assumptions

The basic assumptions underlying PA-theory in its most recent presentation may be formulated as follows:

(i) The primary step of thermal decomposition consists in the congruent dissociative evaporation of reactant.
(ii) Primary decomposition products may differ of those at equilibrium.
(iii) Part (τ) of the energy evolved in the process of condensation of low-volatile product in the reaction interface is consumed by the reactant as a fraction of the enthalpy change.

2.2. Decomposition rate and the Hertz–Langmuir equation

In case of a reactant R decomposed in vacuum into gaseous products A and B with simultaneous condensation of low-volatility species A, i.e.:

$$\mathrm{R(s)} \rightarrow a\mathrm{A(g)}\downarrow + b\mathrm{B(g)} \tag{1}$$

the flux of each product, which ultimately determines the maximum rate of decomposition, can be expressed through the so-called equivalent partial pressure P_{eq} (bar) of this product corresponding to the hypothetical equilibrium of reaction (1) in a general form [13]:

$$J = \frac{\gamma M P_{\mathrm{eq}}}{(2\pi MRT)^{1/2}} \tag{2}$$

where M is the molar mass of product. Here $\gamma = 10^5\,\mathrm{Pa\,bar^{-1}}$ is the conversion factor from bars used to calculate partial pressures in chemical thermodynamics to pascals. This relationship is usually called the Hertz–Langmuir equation.

2.3. Equilibrium pressure of product for dissociative evaporation

The partial pressure, P_{A}, of product A can be calculated from the equilibrium constant, K_P, for reaction (1). In the absence of reaction products in the reactor atmosphere, the situation corresponding to the *equimolar* evaporation mode, the partial pressure P_{A} can be expressed [13] as

$$P_{\mathrm{A}}^{\mathrm{e}} = a\left(\frac{K_P}{F}\right)^{1/\nu}\left(\frac{M_{\mathrm{A}}}{M_{\mathrm{B}}}\right)^{b/2\nu} = \frac{a}{F^{1/\nu}}\left(\frac{M_{\mathrm{A}}}{M_{\mathrm{B}}}\right)^{b/2\nu}\exp\frac{\Delta_{\mathrm{r}}S_T^\circ}{\nu R}\exp\left(-\frac{\Delta_{\mathrm{r}}H_T^\circ}{\nu RT}\right) \tag{3}$$

where

$$F \equiv a^a \times b^b \tag{4}$$

$$\nu = a + b \tag{5}$$

and

$$K_P = P_{\mathrm{A}}^a \times P_{\mathrm{B}}^b \tag{6}$$

where $\Delta_{\mathrm{r}}H_T^\circ$ and $\Delta_{\mathrm{r}}S_T^\circ$ are, respectively, the changes of the enthalpy and entropy in reaction (1).

If the partial pressure P'_{B} of the gaseous component B greatly exceeds the equivalent pressure of the same component released in the decomposition and if, in addition to that, the magnitude of remains constant in the process of decomposition, we call such an evaporation mode *isobaric*. In this case:

$$P_{\mathrm{A}}^{\mathrm{i}} = \frac{K_P^{1/a}}{(P'_{\mathrm{B}})^{b/a}} = \frac{1}{(P'_{\mathrm{B}})^{b/a}}\exp\frac{\Delta_{\mathrm{r}}S_T^\circ}{aR}\exp\left(-\frac{\Delta_{\mathrm{r}}H_T^\circ}{aRT}\right) \tag{7}$$

Eqs. (2)–(7) can be used for the calculation of the main parameters determining the kinetics of sublimation/decomposition processes: the evaporation rate J and two traditional Arrhenius parameters, entering the Arrhenius equation:

$$k = A\exp\left(-\frac{E}{RT}\right) \tag{8}$$

As can be seen from Eqs. (3)–(8), the E parameter for reaction (1) should be different for the equimolar and isobaric modes of decomposition, i.e.:

$$E^{\mathrm{e}} = \frac{\Delta_{\mathrm{r}}H_T^\circ}{\nu} = \frac{\Delta_{\mathrm{r}}H_T^\circ}{a+b} \tag{9}$$

for the equimolar mode and

$$E^{\mathrm{i}} = \frac{\Delta_{\mathrm{r}}H_T^\circ}{\nu - b} = \frac{\Delta_{\mathrm{r}}H_T^\circ}{a} \tag{10}$$

for the isobaric mode. In the former case, the E parameter corresponds to the enthalpy of the decomposition reaction reduced to one mole of all primary products or to the *molar enthalpy*, and in the latter case, to the enthalpy of the decomposition reaction reduced to one mole of primary products without including components of that present in excess.

Interpretation of the physical meaning of the E parameter is a central part of ideology in kinetics of solid decomposition. This quantity is usually interpreted as the energy barrier on the way of reaction and its magnitude in majority of cases is proposed to be higher than the enthalpy change for imaginary equilibrium reaction. This is not the case. As shown above, the value of the E parameter is actually the molar enthalpy of the real reaction (Fig. 1).

2.4. Calculation of the entropy and enthalpy of decomposition reaction

The entropy change for decomposition reaction (1) is calculated from the obvious equation:

$$\Delta_{\mathrm{r}}S_T^\circ = aS_T^\circ(\mathrm{A}) + bS_T^\circ(\mathrm{B}) - S_T^\circ(\mathrm{R}) \tag{11}$$

Calculation of the enthalpy change is more complicated. In order to take into account the partial transfer of the energy released in the condensation of low-volatility product A to the

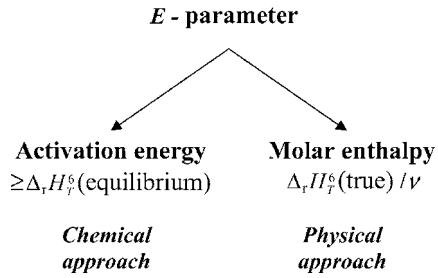

Fig. 1. Interpretation of the E parameter in different approaches. The symbols $\Delta_r H^\circ_T$ (equilibrium) and $\Delta_r H^\circ_T$ (true) correspond to the enthalpies of ideal equilibrium and real decomposition reactions, respectively.

reactant, we introduced into calculations of the enthalpy of decomposition reaction (1) an additional term $\tau a \Delta_c H^\circ_T(\mathrm{A})$, where the coefficient τ corresponds to the fraction of the condensation energy consumed by the reactant. Thus, we can write

$$\begin{aligned}\Delta_r H^\circ_T &= a\Delta_f H^\circ_T(\mathrm{A}) + b\Delta_f H^\circ_T(\mathrm{B}) \\ &\quad - \Delta_f H^\circ_T(\mathrm{R}) + \tau a \Delta_c H^\circ_T(\mathrm{A}) \\ &= \Delta_{vap} H^\circ_T + \tau a \Delta_c H^\circ_T(\mathrm{A}) \end{aligned} \tag{12}$$

where $\Delta_{vap} H^\circ_T$ is the enthalpy of the dissociative vaporization only.

Taking into account Eqs. (9) and (12), we obtain:

$$\begin{aligned}\tau &= \frac{\nu E - a\Delta_f H^\circ_T(\mathrm{A}) - b\Delta_f H^\circ T(\mathrm{B}) + \Delta_f H^\circ_T(\mathrm{R})}{a\Delta_c H^\circ_T(\mathrm{A})} \\ &= \frac{\nu E - \Delta_{vap} H^\circ_T}{a\Delta_c H^\circ_T(\mathrm{A})} \end{aligned} \tag{13}$$

As was revealed recently [7,9], the τ parameter varies for different reactants and is in correlation with the reduced value of condensation energy, $\Delta_c H^\circ_T/RT$, at decomposition temperature (see Section 4.3).

3. The third-law method

3.1. The principle of the method

The third-law method is based on the direct application of the basic equation of chemical thermodynamics:

$$\Delta_r H^\circ_T = T(\Delta_r S^\circ_T - R \ln K_P) \tag{14}$$

where, as before, K_P is the equilibrium constant for the reaction (1). Taking into account Eqs. (5), (6), (9) and (10), Eq. (14) in the case of decomposition of reactant in vacuum can be reduced to the equation:

$$E^{\mathrm{e}} = T\left(\frac{\Delta_r S^\circ_T}{\nu} - R \ln P_{\mathrm{eq}}\right) \tag{15}$$

for the equimolar mode and to the equation:

$$E^{\mathrm{i}} = T[\Delta_r S^\circ_T - R \ln(P_{\mathrm{eq}} P'_{\mathrm{B}})] \tag{16}$$

for the isobaric mode (at $a = b = 1$), where P'_{B} is the external pressure of gaseous product B.

The equivalent pressure of the gaseous product is related to the total absolute rate of decomposition, J (kg m^{-2} s^{-1}), by the Hertz–Langmuir equation (2) rewritten as

$$P_{\mathrm{eq}} = \frac{(2\pi \bar{M} RT)^{1/2} J}{\gamma M_{\mathrm{B}}} \tag{17}$$

Here $\bar{M}$ is the geometrical mean for molar masses of products or

$$\bar{M} = (M^a_{\mathrm{A}} \times M^b_{\mathrm{B}})^{1/(a+b)} \tag{18}$$

3.2. Operating conditions

As it follows from consideration of Eq. (15), using the third-law method for determination of the E parameter assumes a possibility of evaluation of the equivalent pressure, P_{eq}, in conditions of free-surface decomposition of reactant and the availability of data necessary for calculation of the molar entropy of reaction, $\Delta_r S^\circ_T/\nu$. In its turn, calculation of P_{eq} value from the Hertz–Langmuir equation assumes a possibility of measuring the absolute rate of decomposition, J (kg m^{-2} s^{-1}), what suggests a possibility for evaluation of the efficient surface area of decomposed sample. Let us consider these topics in more detail.

3.2.1. Free-surface decomposition

Condition of free-surface decomposition means the absence of any diffusion limitations for the escape of gaseous product from the surface of decomposed sample. This condition is usually referred to high vacuum in the reactor ($<10^{-8}$ bar). However, in many cases, this prerequisite is too high (superfluous). It is easy to estimate an allowable level for the presence of foreign (inert) gas in the reactor if to compare the decomposition rate in high vacuum described by Eq. (2) with the decomposition rate in the presence of inert gas described by one-dimensional diffusion equation [13]:

$$J = \frac{\gamma M D P_{\mathrm{eq}}}{zRT} \tag{19}$$

Here D is the coefficient of diffusion of product vapors in inert gas and z the distance from the vaporization surface to the sink, where the concentration of product vapors drops to zero. The presence of inert gas can be neglected if

$$\frac{\gamma M D P_{\mathrm{eq}}}{zRT} \geq \frac{\gamma M P_{\mathrm{eq}}}{(2\pi MRT)^{1/2}} \tag{20}$$

That means that

$$D \geq z\left(\frac{RT}{2\pi M}\right)^{1/2} \tag{21}$$

If we further take into account that [14]

$$D \cong D_0 \frac{P_0}{P}\left(\frac{T}{T_0}\right)^{1.8} \tag{22}$$

where $P_0 = 1$ bar, $T_0 = 273$ K and $D_0 \cong 2 \times 10^{-5}$ m^2 s^{-1} (for O_2, CO, CO_2 and H_2O diffusion in argon, air or nitrogen [14]) and assume that $M = 0.05$ kg mol^{-1} and $z = 4$ mm $= 4 \times 10^{-3}$ m (the height of a crucible with sample), then allowable pressure, P, of inert gas in the reactor can be evaluated from the relationship:

$$P \leq 4 \times 10^{-8} T^{1.3} \quad (23)$$

It can be seen from Eq. (23) that $P \cong 3 \times 10^{-4}$ bar at 1000 K and 2×10^{-4} bar at 700 K. This means that in many cases the condition of free-surface decomposition can be achieved at evacuation of reactor with only a rotation pump. For illustration, the rate of decomposition of dolomite at 800 K is practically identical (2.3×10^{-5} and 1.8×10^{-5} kg m^{-2} s^{-1}) at residual pressure of air, respectively, 2×10^{-4} and 8×10^{-8} bar [3]. (A small increase of the rate in low vacuum is related to reduction of the self-cooling effect. This topic will be discussed in detail below.)

3.2.2. Absolute rate of decomposition

For application of the third-law method to the determination of the E parameter, it is necessary to know the absolute rate of sample decomposition J (kg m^{-2} s^{-1}). For crystals or pressed pellets with a low porosity, the effective surface area of decomposition could be evaluated from the known geometry of samples. The evaluation of the efficient surface area of powders with the undefined grain size and number of particles presents a serious problem. In principle, the application of the BET technique permits to determine this value. However, the decomposition of powders is not spatially homogeneous. Because of the self-cooling effect, the temperature of inner parts of the powder is lower than that of the surface. This fact was noted in many works though no one tried to investigate this problem quantitatively.

L'vov et al. [15,16] proposed a fairly simple theoretical model and developed a program to compute the temperature of individual crystals and the layer-by-layer temperature distribution in powder samples during the course of their decomposition in vacuum and in the presence of foreign gases. It is suggested that the heat expended in decomposing a sample in a stationary regime is compensated by the radiation emitted by the heater (a crucible) and powder grains and through heat transfer by the gas molecules. Simulation of the temperature distribution, inside a powder sample, can be reduced to modeling the vertical distribution between horizontal layers of this material of thickness equal to the powder grain diameter. If the furnace temperature is the same on top and at the bottom of the sample, the analysis can be limited to considering only one-half of such multilayered sample, from the central, zeroth or first layer, to the nth outermost layer. All the calculations are performed with the laboratory-developed computer program described in [16].

In addition to the temperature distribution, the program permits to calculate simultaneously the quantity n_e corresponding to the effective number of powdered sample layers whose decomposition occurs at the same rate as that of the surface layer.

Such calculations have been performed by L'vov and Ugolkov [3] for the decomposition of dolomite (crystals and powders) in high and low vacuum as a function of a total number of powder layers ($n = 10$ and 100) and values of the emittance parameter ($\varepsilon = 1$, 0.3, 0.1, 0.03 and 0.01). The following conclusions were deduced from the analysis of these data:

1. In all cases, the self-cooling effect is increased with reducing of the emittance parameter. The effect is more pronounced for powders compared to crystals.
2. The self-cooling effect in low vacuum ($P_{air} = 2 \times 10^{-4}$ bar) is much smaller than that in high vacuum ($P_{air} < 3 \times 10^{-7}$ bar).
3. The difference in the grain size and mass of a powder sample (n values) has practically no effect on the temperature distribution and the effective number of powdered sample layers (n_e) whose decomposition occurs at the same rate as that of the surface layer.
4. The difference in the decomposition rates for powders and a crystal is not very high. In the range of the ε parameter from 0.01 to 0.3, this difference is within a factor of 2 or smaller.

The last conclusion is extremely important for application of the third-law method to the calculation of the E parameter in cases of powder samples. It means that, irrespective of the differences in temperature and surface area between powders and crystal, the absolute rate of powder decomposition can be approximately estimated taking into account only the outer surface area of powdered sample. This value can be easily evaluated from the geometry (diameter) of the crucible and the thickness of powder layer in the crucible.

The above theoretical conclusions were verified experimentally on different samples of dolomite taken in the form of natural crystals and powders [3]. The absolute rate of decomposition for powders (J_p) in all cases was higher than that for the crystals (J_c) and, as was shown, the difference in the decomposition rates for powders and crystals is rather constant and does not depend on the temperature, residual pressure of air in the reactor, the mass of powder samples and the size of grains. The mean value of the ratio J_p/J_c at different temperatures is equal to 2.8 ± 0.4. This magnitude is a bit higher than that expected from the model calculations. Most probably, this is related with the uneven surface of layers of powder. In particular, the surface formed by spherical particles is about twice in area compared with that for a flat surface. It might be higher than twice for grains with the irregular shape.

Based on above results, a simple procedure was proposed for determination of the E parameter by the third-law method from the data obtained for powder samples [3]. It consists in evaluation of the absolute decomposition rate of a powder sample (reduced to the unit of the outer surface area of a pellet formed by the powder sample in a cylindrical

crucible). The value received is lowered by the empirical factor and then used for the calculation of the E parameter by the third-law method. The magnitude of this factor (2.8 ± 0.4), as noted above, does not depend on the temperature, residual pressure of air in the reactor, grain size and mass of a powder sample though its constancy for any one of different reactants deserves further investigation. This procedure permitted to greatly expand the application of the third-law method to the determination of decomposition kinetics for many solids available only in the powder form [3–12].

The similar technique can be applied to investigation of melts. To eliminate spreading of melt over the surface of crucible in the process of heating, a mixture of reactant with some neutral powder (e.g., Al_2O_3) taken in the ratio of 1 to 1 is used. After melting of reactant, such mixture retains the powder structure of Al_2O_3 so that evaluation of the absolute decomposition rate remains identical to that described above. The technique was applied to melted Ag and Cd nitrates [10]. Equality of absolute rates of decomposition for mixtures of melted $AgNO_3$ and Al_2O_3 taken in different ratios (1:1 and 1:5) supported this scheme of calculation.

3.2.3. Entropy change

The availability of data necessary for calculation of the molar entropy of reaction, $\Delta_r S_T^\circ/\nu$, is at first glance a serious limitation for application of the third-law method. Fortunately, the situation in this field is significantly improved over the last 40 years and for majority of substances the values of entropies in standard conditions (S_{298}°) and corresponding temperature increments ($S_T^\circ - S_{298}^\circ$)were calculated and published in tabulated form in many handbooks (as an example, in [17–20] in Russia). Nevertheless, in some cases, for example, for low-volatility molecules in the gaseous state (e.g., metal salts), these data are absent. In some cases, it is possible to estimate the entropy value from a comparison with the known entropies of similar molecules for other metals. This approach was used, for example, for gaseous molecules of Li_2SO_4, $CaSO_4$ and $CuSO_4$ [4].

More general approach for estimation of molar entropy was demonstrated in [1]. Instead of true values of $\Delta_r S_T^\circ/\nu$ for 20 different reactants, their average magnitude ($148 \pm 17\,J\,mol^{-1}\,K^{-1}$) was used for all these reactants. The correlation between the E parameters and the molar enthalpies for corresponding decomposition reactions was a bit worse for the approximate version: the mean value of R.S.D. was 5% compared with 3% for the precise version.

Our recent analysis of $\Delta_r S_T^\circ/\nu$ values for 50 different reactants has revealed significant differences in $\Delta_r S_T^\circ/\nu$ between the reactants decomposed with formation of free metal atoms and reactants decomposed up to metal products in the form of free molecules. As can be seen from Tables 1 and 2, the average value of $\Delta_r S_T^\circ/\nu$ is equal to $136 \pm 9\,J\,mol^{-1}\,K^{-1}$ in the first case and to $160 \pm 9\,J\,mol^{-1}\,K^{-1}$, in the second. In both cases, R.S.D. values are only one-half its value for all 50 reactants. As will be shown later (Section 4.5), under these circumstances, the approximate and precise versions of calculation of the E parameter are not distinguished in precision.

Table 1
The molar entropy for decomposition reactions at $P_{eq} \cong 10^{-7}$ bar (metal products are in the form of free atoms) [17–20]

Decomposition reaction	T (K)	$\Delta S_T^\circ/\nu$ ($J\,mol^{-1}\,K^{-1}$)[a]
$FeO \rightarrow Fe + 1/2O_2$	1200	130.0
$CoO \rightarrow Co + 1/2O_2$	1100	140.0
$NiO \rightarrow Ni + 1/2O_2$	925	152.0+
$MgO \rightarrow Mg + 1/2O_2$	1600	137.9
$MnO \rightarrow Mn + 1/2O_2$	1600	127.3
$Cu_2O \rightarrow 2Cu + 1/2O_2$	800	128.0
$CdO \rightarrow Cd + 1/2O_2$	1300	129.0
$HgO \rightarrow Hg + O$	680	129.0
$ZnO \rightarrow Zn + O$	1260	134.1
$CdS \rightarrow Cd + 1/2S + 1/4S_2$	1000	127.5
$CdSe \rightarrow Cd + 1/2Se + 1/4Se_2$	1000	123.9−
$ZnS \rightarrow Zn + 1/2S + 1/4S_2$	1000	131.2
$ZnSe \rightarrow Zn + 1/2Se + 1/4Se_2$	1000	121.5−
$Be_3N_2 \rightarrow 3Be + N + 1/2N_2$	1600	135.1
$Mg_3N_2 \rightarrow 3Mg + N + 1/2N_2$	1000	131.3
$BN \rightarrow B + 1/2N_2$	1800	154.7+
$AlN \rightarrow Al + 1/2N + 1/4N_2$	1800	148.5+
$GaN \rightarrow Ga + 1/2N + 1/4N_2$	1200	135.3
$InN \rightarrow In + 1/2N + 1/4N_2$	1120	138.3
$Si_3N_4 \rightarrow 3Si + 2N + N_2$	1700	155.3+
$NaN_3 \rightarrow Na + N + N_2$	300	133.8
$KN_3 \rightarrow K + N + N_2$	300	133.6
$Pb(N_3)_2 \rightarrow Pb + N + N_2 + N_3$	300	141.9
$AgNO_3(l) \rightarrow Ag + NO_2 + 1/2O_2$	570	128.5
$AgNO_3 \rightarrow Ag + NO_2 + 1/2O_2$	480	142.4
Average ± S.D. ($n = 25$)		136 ± 9

[a] The $\Delta S_T^\circ/\nu$ values outside $136 \pm 9\,J\,mol^{-1}\,K^{-1}$ interval are denoted by marks: − or +.

3.3. Precision

As can be seen from the analysis of results reported in [17] for several hundreds of substances (mainly related to their enthalpies of formation or sublimation) and the results of recent application of third-law method to the determination of the E parameter for many decomposition reactions [1–12], the data calculated by the third-law method are in general the order of magnitude more precise than those calculated by the second-law method and Arrhenius-plots methods. This is connected with the different impact of systematic and random errors in the determination of the true temperature of reactant and J, P or k variables on ΔH_T° or E values. It is clear if we compare Eqs. (14)–(16) with Eq. (24) valid in cases of the second-law and Arrhenius-plots methods:

$$\Delta H_T^\circ = \frac{1}{T_{min}^{-1} - T_{max}^{-1}} R \ln \frac{P_{max}}{P_{min}} = \frac{T_{max} T_{min}}{T_{max} - T_{min}} R \ln \frac{P_{max}}{P_{min}} \quad (24)$$

where P_{max} and P_{min} are, respectively, the partial pressures at the maximum (T_{max}) and minimum (T_{min}) temperatures

Table 2
The molar entropy for decomposition reactions at $P_{eq} \cong 10^{-7}$ bar (metal products are in the form of free molecules) [17–20]

Decomposition reaction	T (K)	$\Delta S_T^\circ/\nu$ ($J\,mol^{-1}\,K^{-1}$)[a]
$2P\ (red) \rightarrow P_2$	600	162.3
$6As \rightarrow As_4 + As_2$	550	157.3
$6Sb \rightarrow Sb_4 + Sb_2$	650	152.9
$GeO_2 \rightarrow GeO + 1/2O + 1/4O_2$	1300	167.9
$SnO_2 \rightarrow SnO + O$	1240	160.7
$Pb_3O_4 \rightarrow 3PbO + O$	700	153.7
$Be(OH)_2 \rightarrow BeO + H_2O$	395	169.1+
$Mg(OH)_2 \rightarrow MgO + H_2O$	530	163.0
$Ca(OH)_2 \rightarrow CaO + H_2O$	570	153.5
$Sr(OH)_2 \rightarrow SrO + H_2O$	595	151.7
$Ba(OH)_2 \rightarrow BaO + H_2O$	600	140.0−
$Zn(OH)_2 \rightarrow ZnO + H_2O$	380	168.2
$Cd(OH)_2 \rightarrow CdO + H_2O$	400	164.3
$MgCO_3 \rightarrow MgO + CO_2$	670	174.8+
$CaMg(CO_3)_2 \rightarrow CaO + MgO + 2CO_2$	800	166.0
$CaCO_3 \rightarrow CaO + CO_2$	860	158.0
$SrCO_3 \rightarrow SrO + CO_2$	910	161.0
$BaCO_3 \rightarrow BaO + CO_2$	1060	142.0−
$MgSO_4 \rightarrow MgO + SO_2 + O$	1010	171.0+
$BaSO_4 \rightarrow BaO + SO_2 + O$	1390	152.0
$Cd(NO_3)_2 \rightarrow CdO + 2NO_2 + O$	550	163.0
$Pb(NO_3)_2 \rightarrow PbO + 2NO_2 + O$	530	160.0
$Li_2SO_4{\cdot}H_2O \rightarrow Li_2SO_4 + H_2O$	300	175.9+
$CaSO_4{\cdot}2H_2O \rightarrow CaSO_4 + 2H_2O$	310	159.8
$CuSO_4{\cdot}5H_2O \rightarrow CuSO_4 + 5H_2O$	290	159.1
Average ± S.D. ($n = 25$)		160 ± 9

[a] The $\Delta S_T^\circ/\nu$ values outside $160 \pm 9\,J\,mol^{-1}\,K^{-1}$ interval are denoted by marks: − or +.

of the experiment (in case of the Arrhenius-plots method, the rate constants, k, or absolute rates, J, are usually used in place of P values). Instead of a proportional dependence of the error in ΔH_T° (or the E parameter) determination on the error of T in case of the third-law method, the error in ΔH_T° determination is proportional to the error in the slope of the plot in cases of the second-law and Arrhenius-plots methods. As can be seen from comparison of Eq. (24) with Eqs. (14)–(16), this leads to $T_{max}/(T_{max} - T_{min})$ increase of error.

Under rather typical measurement conditions, e.g., at $T_{min} = 900\,K$ and $T_{max} = 1000\,K$, an error of 10 K because of the self-cooling effect (i.e., at $T_{max} = 990\,K$ instead of 1000 K) results in the error in ΔH_T° calculation about 9% instead of only 1% in case of the third-law method applied at T_{max}. Furthermore, as can be seen from Eq. (15), a twofold difference in the absolute rate of decomposition can introduce $5.2\,kJ\,mol^{-1}$ error in the determination of the E parameter at 900 K by the third-law method. In case of the Arrhenius-plots method (Eq. (24)), a twofold difference in the ratio P_{max}/P_{min} (or k_{max}/k_{min}) should introduce $52\,kJ\,mol^{-1}$ error in the determination of the E parameter (at $T_{min} = 900\,K$ and $T_{max} = 1000\,K$). Therefore, precision of the third-law method is, on the average, the order of magnitude higher than that of the second-law and Arrhenius-plots methods. But the difference may be even more dramatic. There are some reports in the literature when the ratio $T_{max}/(T_{max} - T_{min})$ and resultant difference in precision reaches a factor of 30–50.

If reproducibility in measurements of rates of decomposition is within of factor 2 (this assumption is supported by our experience), relative deviations of the E parameter should be lower than 2%. This follows from the analysis of Eq. (15) if to take into account the average values of $\Delta_r S_T^\circ/\nu$ and $R \ln P_{eq}$ (148 and $134\,J\,mol^{-1}\,K^{-1}$, respectively).

3.4. Time spent for the experiment

The application of the third-law method at only one temperature greatly reduces (by a factor of 10 or more) the total time spent for the experiment in comparison with that for the second-law and Arrhenius-plots methods. This is easy to understand by considering the total number of points usually used for plotting. Most of the workers who applied the second-law and Arrhenius-plots methods under isothermal measurement conditions used, by our estimation [1], from 10 to 60 points. Even in the non-isothermal experiments, at least three heating rates are recommended in order to correctly describe the course of reaction. In case of the third-law method, a single measurement of the decomposition rate takes entirely not more than 2–3 h.

4. Applications

4.1. The initial decomposition temperature and the E parameter

The first application of the third-law method to the thermal decomposition of solids was related to investigation of the interrelation between the initial temperature of decomposition and the E parameter [1]. As follows from Eq. (15), the ratio of these quantities is equal to

$$\frac{T}{E^e} = \frac{1}{\Delta S_T^\circ/\nu - R \ln P_{eq}} \tag{25}$$

It happened that for different instrumental techniques and different experimental conditions used in kinetic investigations, the reported initial temperatures of decomposition, T_i, correspond, with rare exceptions, to the partial pressure of gaseous products of about 10^{-7} bar (within of factor of 10 in both directions). This item has been discussed in [1]. The averaged value of molar entropy is equal to $148 \pm 17\,J\,mol^{-1}\,K^{-1}$ (Section 3.2.3). Therefore, the T_i/E^e ratio can be presented ($K\,kJ^{-1}$ mol) as

$$\frac{T_i}{E^e} = \frac{1000}{(148 \pm 17) + (134 \pm 19)} = \frac{1000}{282 \pm 25} = 3.5 \pm 0.3 \tag{26}$$

To compare this theoretical prediction with experiment, L'vov [1] collected available T_i/E^e values reported in the lit-

erature. Different types of reactants were used for comparison: from some metalloids (As and Sb) and simple binary compounds (oxides, sulfides, selenides, nitrides, carbides and borides) to metal salts of inorganic and organic acids (nitrates, sulfates, carbonates, permanganates, formates, acetates and oxalates), and hydrated salts. Some explosive substances (azides, ammonium salts, tetryl, metal styphnates and nitrogen iodide) were included as well. The initial decomposition temperatures for these substances range from 253 K for nitrogen iodide to 2973 K for TaC. In all cases, the experiments were performed in vacuum or an inert atmosphere, i.e., in the absence of primary gaseous products in the reactor (the equimolar mode of evaporation).

These data were arranged into two groups. The first group contained the results for the decompositions of 50 substances into gaseous products only and the second group, for the decompositions of 50 compounds into gaseous and solid products. The distribution of T_i/E^e values for all 100 reactants is shown in Fig. 2. Each point of this distribution was calculated within steps of equal increment (0.2) in T_i/E^e ratio. The distribution is rather close to the Gaussian curve. This is in agreement with a random origin of errors.

As has been deduced from the analysis of these results [1], the average value of the ratio T_i/E^e ($3.6 \pm 0.4\,\mathrm{K\,kJ^{-1}\,mol}$) practically coincides with its theoretical value. No difference was observed between the mean T_i/E^e values for reactants decomposed into gaseous products only and those ultimately decomposed to yield solid and gaseous products. All the above strongly supports the validity of the concepts that form the bases of Eq. (25), i.e., the dissociative evaporation mechanism of decomposition and the equality

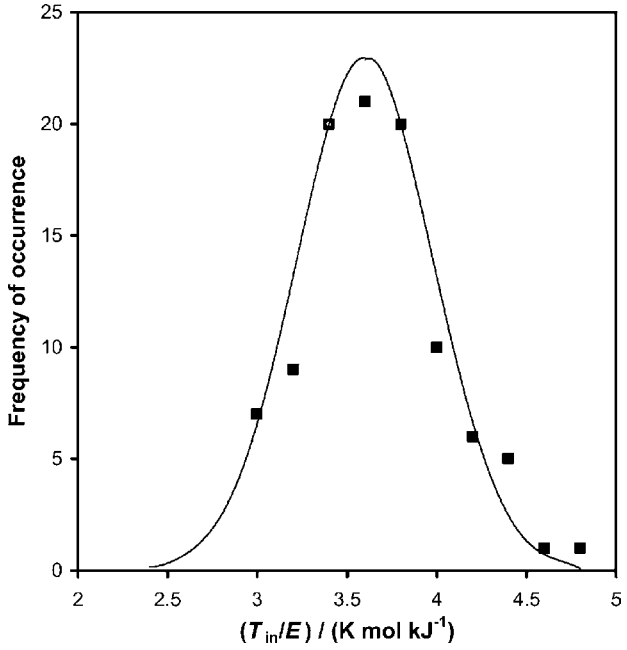

Fig. 2. The frequency of occurrence of T_i/E values in steps of equal increment (0.2). A total of 100 values are included [1]. The curve corresponds to the Gaussian distribution.

of the E parameter to the molar enthalpy of corresponding reaction.

4.2. Carbonate decomposition in CO_2

The peculiarities of thermal decomposition of alkaline earth carbonates in atmosphere of CO_2 were studied over the last 70 years in many works. However, there is no agreement in quantitative and even in qualitative interpretation of kinetics for this reaction [6]. In most of the publications, increase of CO_2 pressure is accompanied by increase of the E parameter, which in some cases reached 2000–4000 $\mathrm{kJ\,mol^{-1}}$. At the same time, the peculiarities of thermal decomposition of carbonates in atmosphere of CO_2 can be used as a very convincing argument pro et contra one or other mechanism of decomposition, in particular, the mechanism of thermal decomposition based on the primary dissociative evaporation of reactant with simultaneous condensation of the low-volatile product. Assuming the validity of this mechanism, two important consequences can be deduced from the above theoretical discussion (Section 2):

1. The value of the E parameter for decomposition of carbonates in the presence of CO_2 (the isobaric mode) should be invariant with respect to the partial pressure of CO_2, P'_{CO_2}. This follows from consideration of Eqs. (2) and (7) defined the temperature dependence of the decomposition rate.
2. The values of the E parameter for solid decomposition in the presence of gaseous product B (the isobaric mode) and in its absence (the equimolar mode) should be subjected to the relation:

$$E^i = \left(\frac{\nu}{a}\right) E^e \tag{27}$$

and in case of carbonate decomposition (when $a = 1$ and $\nu = 2$), to the relation:

$$E^i = 2E^e \tag{28}$$

When the experimental results obtained in [6] and reported in the literature are compared with these theoretical predictions, it becomes apparent that they are in excellent agreement. First, the values of the E parameters for decomposition of $CaCO_3$ (Table 3) and $SrCO_3$ (Table 4) in the presence of CO_2 are invariant with respect to the partial pressure of CO_2 varied in the range of 4–5 orders of magnitude. Secondly, the values of the E parameter for decomposition $CaCO_3$, $SrCO_3$ and $BaCO_3$ in the presence and in the absence of CO_2 (Table 5) are subjected to the theoretically predicted relation (28). The averaged value E^i/E^e is equal to 1.98 ± 0.03 instead of 2.00. It could not be better. Note that Beruto et al. [21] reported recently the value of $E^i = 440 \pm 10\,\mathrm{kJ\,mol^{-1}}$ for decomposition of natural dolomite powder in atmosphere of CO_2, which is of factor 1.8 higher than the value $E^e = 246 \pm 1\,\mathrm{kJ\,mol^{-1}}$ measured in vacuum by L'vov and Ugolkov [3].

Table 3
Values of the E parameter for $CaCO_3$ decomposition in the presence of CO_2 calculated by the third-law method [6]

Atmosphere	P'_{CO_2} (bar)	T (K)	P_{eq} (bar)	ΔS°_T (J mol^{-1} K^{-1})	E (kJ mol^{-1})[a]
N_2 (dry)	2.0×10^{-1}	1123	4.75×10^{-7}	307.2	496.0
N_2 (dry)	6.0×10^{-1}	1173	9.70×10^{-7}	305.8	498.7
N_2 (dry)	5.4×10^{-1}	1223	5.00×10^{-6}	304.2	502.4
Vacuum	1.0×10^{-4}	898	5.10×10^{-8}	314.6	493.8
Vacuum	1.0×10^{-3}	983	8.00×10^{-8}	311.9	496.6
Vacuum	1.0×10^{-3}	1006	1.08×10^{-7}	311.3	505.1
He (8 mbar)	3.6×10^{-6}	857	2.23×10^{-8}	316.1	485.7
He (8 mbar)	1.5×10^{-5}	897	5.60×10^{-8}	314.6	489.8
He (8 mbar)	4.0×10^{-5}	935	1.49×10^{-7}	313.4	494.0
He (8 mbar)	5.8×10^{-5}	954	2.46×10^{-7}	312.8	496.5
He (8 mbar)	7.8×10^{-5}	974	4.86×10^{-7}	312.2	498.4
Ar	1.0×10^{-1}	1100.3	9.05×10^{-7}	308.0	487.3
Ar	1.0×10^{-1}	1071.0	1.30×10^{-7}	308.9	492.5
Ar	1.0×10^{-1}	1070.9	1.80×10^{-7}	308.9	489.3
Average		1020 ± 110			495 ± 6

[a] Calculated by Eq. (16).

Table 4
Values of the E parameter for $SrCO_3$ decomposition in the presence of CO_2 calculated by the third-law method [6]

Atmosphere	P'_{CO_2} (bar)	T (K)	P_{eq} (bar)	$\Delta_r S^\circ_T$ (J mol^{-1} K^{-1})	E (kJ mol^{-1})[a]
Vacuum	3.9×10^{-5}	1003	6.4×10^{-9}	318.9	562
Vacuum	2.2×10^{-4}	1053	5.0×10^{-9}	317.0	575
Vacuum	1.3×10^{-3}	1133	4.7×10^{-8}	314.5	578
Argon	1.0×10^{-1}	1131	5.0×10^{-9}	314.6	557
Argon	1.0×10^{-1}	1151	2.7×10^{-9}	313.9	572
Average		1090 ± 60			569 ± 9

[a] Calculated by Eq. (16).

The agreement of experimental results with theoretical predictions should be considered as a very strong proof of the validity of the primary dissociative evaporation mechanism for carbonate decomposition and the physical approach to the interpretation of kinetics of solid decomposition on the whole. (No other explanation for regularities observed could be proposed). The failure of all the previous investigations into the effect of CO_2 on kinetics of carbonate decomposition may be attributed mainly to shortages of the Arrhenius-plots method and, in case of calcite, to the strong catalytic effect of H_2O vapor on the decomposition rate.

4.3. Correlation between the τ parameter and thermodynamic features of the low-volatility product

The τ parameter was introduced into PA-theory primarily as adjusting factor to correlate the value of E parameter with the molar enthalpy of deduced reaction [22]. That was, on admission of the author himself, "the most weak point of the theory as a whole" [23]. It was assumed [23] that in most cases "the condensation energy is approximately equally divided between the reactant and product phases", so that the τ parameter should be equal to 0.50. However, as it became evident lately, this is not the case. Analysis of variation of τ parameters for eight different reactants (all for alkaline earth metals) made it possible to correlate these values with the supersaturating degree of the low-volatile product (metal oxide) at the moment of decomposition [7]. This correlation was approximated (with the correlation coefficient $r^2 = 0.894$) by the equation:

$$\tau = 0.138 \ln x_1 + 0.03 \quad (29)$$

where $x_1 \equiv \log(P_{eq}/P_{sat})$. Here P_{eq} and P_{sat} are the equivalent and saturation pressures of low-volatile product, respec-

Table 5
Experimental values of the E parameter for carbonate decomposition in the isobaric and equimolar modes [6]

Reaction	T (K)		E (kJ mol^{-1})		E^i/E^e
	Isobaric	Equimolar	Isobaric	Equimolar	
$CaCO_3 \rightarrow CaO(g)_\downarrow + CO_2$	1020	820	495 ± 6	254 ± 6	1.95
$SrCO_3 \rightarrow SrO(g)_\downarrow + CO_2$	1090	908	569 ± 9	286 ± 1.3	1.99
$BaCO_3 \rightarrow BaO(g)_\downarrow + CO_2$	1249	1077	605 ± 1	302 ± 1.5	2.00
Average					1.98 ± 0.03

tively. Recently it has become possible to add to this list of reactants a number of new data for six hydroxides and also for BN [9]. The approximation function:

$$\tau = 0.134 \ln x_1 + 0.07 \quad (30)$$

has not been changed significantly in comparison with Eq. (29), though the range of supersaturating degree, x_1, for all 15 reactants was more than doubled (81.3 against 37.5).

The other possible way for description of the correlation between the τ parameter and thermodynamic characteristics of the low-volatile product was proposed in [9]. The approximation function takes the form:

$$\tau = 0.427 \ln x_2 - 1.49 \quad (31)$$

Instead of the supersaturating degree, $x_1 \equiv \log(P_{eq}/P_{sat})$, the reduced value of condensation energy, $x_2 \equiv \ln(-\Delta_c H_T^\circ/RT)$, was used as a controlling parameter. The correlation coefficient increased in this case from 0.882 up to 0.936. The correlation between τ and x_2 can be improved still further (up to $r^2 = 0.966$) if to approximate this relationship with a quadratic polynomial (Fig. 3):

$$\tau = -0.1312(x_2)^2 + 1.5762x_2 - 3.9757 \quad (32)$$

The correlation revealed should be considered as the most important step in the development of the physical approach as a whole. Now, when it has become possible to evaluate the τ parameter a priori on the basis of the saturation pressure, P_{sat}, or condensation energy, $\Delta_c H_T^\circ$, for the low-volatile product at decomposition temperature, the physical approach gains the features of completed self-consistent theory. But, some questions remain unanswered. The all-important problems consist in the physical interpretation of this correlation and the mechanism of energy consumption by the reactant.

4.4. Decomposition of melted reactants

Tremendous importance for further development of PA-theory is a comparison of the decomposition rates for solid and melted reactants in vacuum. Such comparative experiments have been performed recently by L'vov and Ugolkov [10]. As can be seen from Table 6, in spite of about 100 K difference in temperature, the decomposition rates for $AgNO_3$ in $Cd(NO_3)_2$ in solid and melted states are rather similar. (The difference of the two-three orders of magnitude is expected based on the values of the E parameter.) It means that, on some reasons, the decomposition of solid reactants slows down after their melting. This conclusion is in contradiction to the widespread opinion: "Melting is an important feature in theoretical considerations of crystal reactivity because chemical changes often proceed more rapidly in a melt than in the solid state" [24]. This opinion is based on the following reasonable though, at best, only a priori assumptions: "Reasons why reactions of solids may proceed more rapidly in a molten zone than within a crystalline reactant, include: (i) relaxation of the regular stabilizing intercrystalline forces; (ii) establishment of a favorable configuration for chemical change may be possible due to mobility in a liquid but inhibited within a rigid crystal structure; (iii) the influences of intermediates and impurities may be greater (or different) in a molten phase" [25].

Meanwhile, the retardation effect of melting can be easily explained and quantitatively evaluated in the framework of the physical approach to decomposition kinetics. As stated in [23], the formation of product/reactant interface in the process of solid decomposition with a partial transfer of condensation energy to the reactant ($\tau a \Delta_c H_T^\circ$) reduces the enthalpy of reaction and increases the decomposition rate.

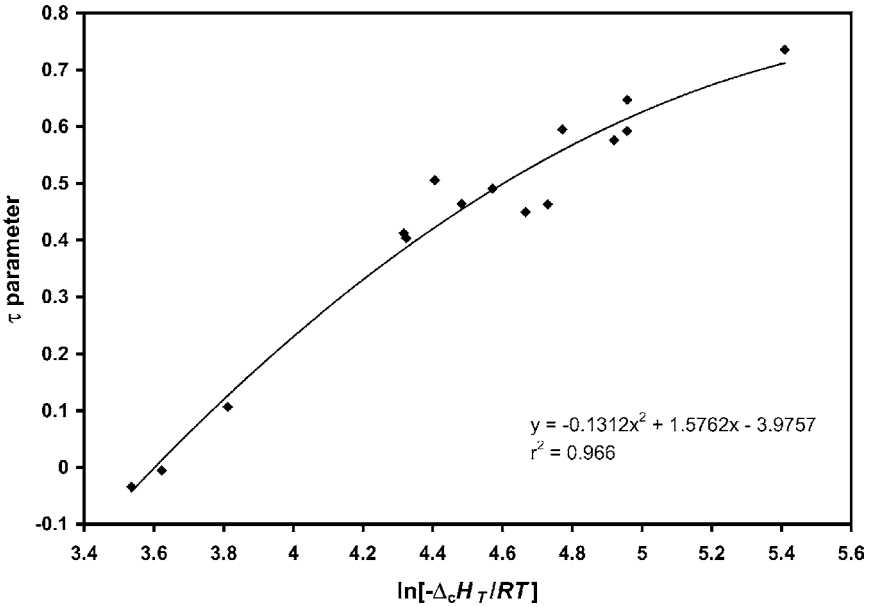

Fig. 3. Dependence of the τ parameter on the condensation energy of low-volatility product at decomposition temperature.

Table 6
The final kinetic parameters for decomposition of solid and melted[a] nitrates [10]

Nitrate	T (K)	J (kg m^{-2} s^{-1})	Primary products[b]	E (kJ mol^{-1})	$\Delta_r H_T^\circ/\nu$ (kJ mol^{-1})
$AgNO_3$(s)	472	3×10^{-7}	$Ag(g)_\downarrow + NO_2 + 1/2O_2$	146.0 ± 0.5	
$AgNO_3$(l)	573	8×10^{-7}	$Ag(g) + NO_2 + 1/2O_2$	164.5 ± 0.6	167.7 ± 1.0
$Cd(NO_3)_2$(s)	563	7×10^{-6}	$CdO(g)_\downarrow + 2NO_2 + O$	174.5 ± 1.5	
$Cd(NO_3)_2$(l)	660	1×10^{-5}	$CdO(g) + 2NO_2 + O$	194.2 ± 0.8	204.3 ± 1.0

[a] The melting points of $AgNO_3$ and $Cd(NO_3)_2$ are equal to 483 and 633 K, respectively.
[b] An arrow (↓) implies taking into account part τ of condensation energy consumed by the reactant.

In the absence of such interface for a liquid reactant, the enthalpy of reaction corresponds to the condition $\tau = 0$. Therefore, the difference in the E parameter for a liquid and solid reactant should be equal to $\tau a \Delta_c H_T^\circ/\nu$. Indeed, the experimental values of the E parameter for liquid and solid $AgNO_3$ (Table 6) differ by the value of $\tau a \Delta_c H_T^\circ/\nu \cong 165 - 146 = 19\,\text{kJ mol}^{-1}$. The corresponding difference in case of $Cd(NO_3)_2$ decomposition is equal to $194 - 174 = 20\,\text{kJ mol}^{-1}$. Now it is easy to understand the reason of the drop of decomposition rate in the moment of $Cd(NO_3)_2$ melting observed by QMS [26].

The results of these comparative experiments for Ag and Cd nitrates are in complete agreement with the results of similar experiments for $Ca(NO_3)_2$ reported by Ettarh and Galwey [27]. The melting point of $Ca(NO_3)_2$ is 836 K. The values of the E parameter measured in [27] for solid (774–820 K) and melted nitrate (229 ± 10 and 315 ± 20 kJ mol^{-1}) are in a good agreement with the results of our calculation of molar enthalpy (234 and 318 kJ mol^{-1}) for corresponding reactions:

$$Ca(NO_3)_2(s) \rightarrow CaO(g)\downarrow + 2NO_2 + O \quad (33)$$

$$Ca(NO_3)_2(l) \rightarrow CaO(g) + 2NO_2 + O \quad (34)$$

The calculated value of $\tau a \Delta_c H_T^\circ/\nu = 84\,\text{kJ mol}^{-1}$ practically coincides with the experimental difference in the E parameter for melted and solid nitrate, i.e., 86 kJ mol^{-1}. The rise of the E parameter for melted $Ca(NO_3)_2$ was left in [27] without comments, though this fact is in obvious contradiction to the concept of increased reactivity of melts advocated by the authors [27]. On the whole, the peculiarities of decomposition of solid and melted nitrates that were discussed above strongly support the basic principles of PA-theory. It needs to be ascertained if these findings are common to decomposition of other reactants, in particular, of some low-melting hydrates.

4.5. Interpretation of decomposition mechanisms

Over many years (starting in 1981 [28]), this author, in agreement with PA-theory, used a comparison of the molar enthalpy, $\Delta_r H_T^\circ/\nu$, of corresponding decomposition reaction with the E parameter of the Arrhenius equation for interpretation of the decomposition mechanism (Fig. 4). However, any impact of this approach on traditional scheme of interpretation of the decomposition mechanisms is practically absent. One possible explanation of this situation might be distrust to the results of comparison of these quantities, which is connected with uncertainty in the values of the E parameter measured by the Arrhenius-plots method. As an example of this distrust, the comment by Vyazovkin [29] can be mentioned: "Note that comparison of theoretical values of the activation energy with the experimental ones may itself present a considerable challenge as the reported values tend to be widely differing".

With a recent introduction of the third-law methodology, the accuracy and precision of measured values of the E parameter were greatly improved. As a rule, the R.S.D. in these measurements is lower than 2%. The same or lower uncertainty can be expected in theoretical values of molar enthalpy, $\Delta_r H_T^\circ/\nu$. By now, the data on the E parameter were accumulated for several classes of reactants popular in TA. Most of them (oxides, nitrides, hydroxides, carbonates, sulfates and nitrates) were measured by L'vov et al. [2–12]. In other cases (P, As, Sb, azides, sulfides, selenides and some nitrides), the primary experimental data reported in the literature (equivalent pressures and/or absolute rates of decomposition) were used for calculation of the E parameters by the third-law method. All these data are collected in Tables 7 and 8. Table 7 contains the corresponding kinetic parameters for reactants decomposed up to the gaseous products and Table 8 contains the same data for reactants ultimately decomposed up to the solid and gaseous products. The values of the E parameter for all reactants were calculated using two approaches. The first of them corresponds

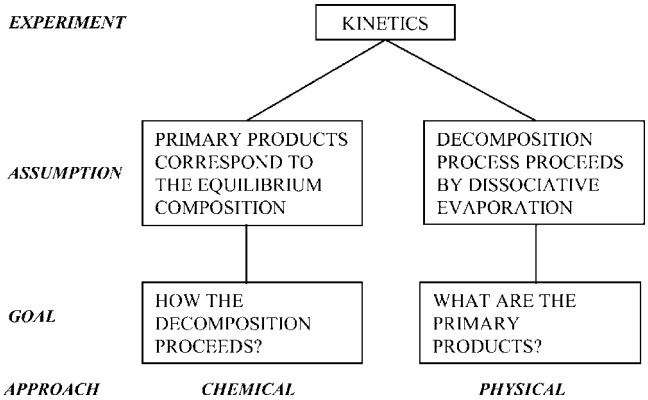

Fig. 4. The simplified schemes for the chemical and the physical approaches to the investigation of decomposition mechanisms.

Table 7
Thermodynamic and kinetic parameters for thermal decompositions of reactants up to the gaseous products

Deduced reaction	ν	T (K)	$\Delta_r H^\circ_T$ (kJ mol^{-1})	$(\Delta S^\circ_T/\nu)$ (J mol^{-1} K^{-1})	P_{eq} (bar)	$\Delta_r H^\circ_T/\nu$ (kJ mol^{-1})	E (kJ mol^{-1})		Reference
							Third-law[a]	Reported	
2P (red) → P_2	1	600	183.5_{600}	162.3_{600}	3.5×10^{-8}	184	183/182	218	[31]
6As → $As_4 + As_2$	2	550	353.9_{600}	157.3_{600}	6.6×10^{-10}	177	183/185	180–183	[31]
6Sb → $Sb_4 + Sb_2$	2	650	429.0_{600}	152.9_{600}	1.3×10^{-9}	214	210/215	207	[31]
GeO_2 → GeO + 1/4O_2 + 1/2O	1.75	1313	650.2_{1300}	167.9_{1300}	8.5×10^{-7}	372	373/363	489	[33]
SiO_2 → SiO + O	2	1754	1040.0_{1800}	155.8_{1800}	8.0×10^{-8}	520	512/519	547	[33]
SnO_2 → SnO + O	2	1239	831.9_{1200}	160.7_{1200}	1.1×10^{-9}	416	412/411	351	[33]
HgO → Hg + O	2	681	401.8_{700}	128.8_{700}	3.0×10^{-8}	201	186/192	162–241	[8]
ZnO → Zn + O	2	1400	724.5_{1400}	133.3_{1400}	2.5×10^{-7}	363	364/367	180–428	[8]
CdSe → Cd + 1/4Se_2 + 1/2Se	1.75	1000	393.4_{1000}	123.9_{1000}	5.4×10^{-6}	225	225/237	234	[33]
ZnS → Zn + 1/4S_2 + 1/2S	1.75	1000	467.2_{1000}	131.9_{1000}	1.0×10^{-7}	267	266/270	258	[33]
ZnSe → Zn + 1/4Se_2 + 1/2Se	1.75	1000	439.6_{1000}	121.5_{1000}	1.7×10^{-7}	251	251/266	294	[33]
AlN → Al + 1/4N_2 + 1/2N	1.75	1700	875.3_{1700}	147.1_{1700}	2.1×10^{-8}	500	500/481	542	[11]
GaN → Ga + 1/4N_2 + 1/2N	1.75	1200	620.3_{1200}	135.3_{1200}	1.4×10^{-8}	354	343/344	305	[11]
InN → In + 1/4N_2 + 1/2N	1.75	1100	602.4_{1100}	138.3_{1100}	5.4×10^{-9}	344	326/324	336	[11]
Be_3N_2 → 3Be + 1/2N_2 + N	4.5	1600	2010.6_{1600}	135.1_{1600}	1.5×10^{-7}	447	425/427	428	[11]
Mg_3N_2 → 3Mg + 1/2N_2 + N	4.5	1200	1356.7_{1200}	130.1_{1200}	1.3×10^{-6}	302	291/298	238	[11]
Si_3N_4 → 3Si + N_2 + 2N	6	1700	3065.1_{1700}	155.3_{1700}	2.4×10^{-8}	511	512/479	480	[11]
NaN_3 → Na + N_2 + N	3	603	550.0_{600}	133.8_{300}	3.4×10^{-8}	183	167/168	144–197	[32]
$AgNO_3$(l) → Ag + NO_2 + 1/2O_2	2.5	574	419.5_{570}	128.5_{570}	5.3×10^{-9}	168	165/169	167–174	[10]
$Cd(NO_3)_2$(l) → CdO + 2NO_2 + O	4	660	817.0_{700}	153.1_{660}	4.0×10^{-8}	204	194/198	186	[10]

[a] First value corresponds to $\Delta S^\circ_T/\nu$ listed in this table, and second value, to the average magnitude of $\Delta S^\circ_T/\nu$: 136 or 160 J mol^{-1} K^{-1} (see Section 3.2.3).

to the true values of molar entropy listed in Tables 7 and 8 and the second, to the average magnitudes of $\Delta_r S^\circ_T/\nu$ (136 or 160 J mol^{-1} K^{-1}) according to the form of metal product (atom or molecule) as discussed in Section 3.2.3.

A comparison of the molar enthalpies of different plausible reactions with the values of the E parameters permitted to choose the composition and stoichiometry of primary products that satisfy the condition $\Delta_r H^\circ_T/\nu \cong E$ or, in other words, to interpret the mechanism of decomposition for 40 different reactants (Tables 7 and 8). For the first time over the century elapsed after a pioneer work by Lewis [30], the decomposition mechanisms of a large group of reactants from different classes of chemical compounds are identified on a single basis. We consider this achievement as the main result of application of the third-law method to decomposition kinetics.

Reliability of the above interpretation is supported by a good correlation between experimental values of the E parameter, on the one hand, and the values of molar enthalpy, $\Delta_r H^\circ_T/\nu$, for the deduced reactions, on the other. The corresponding data are presented in Fig. 5 (for precise version of the third-law method) and in Fig. 6 (for its approximate version). The mean value of relative standard deviation of experimental results (the E parameter) from theoretical values of molar enthalpy for all reactants is 5.6% for precise and 5.1% for approximate version. A small difference in favor of approximate version most likely is accidental. Taking into account errors of the E parameter determination, uncertainty in values of thermodynamic functions and the approximation in a scheme of calculation of τ parameter, agreement is more than satisfactory.

It is important that approximate version of the third-law method provide the same accuracy as the precise version does. This means, in particular, that the approximate version can be used for accurate determination of the E parameters for materials with unknown product composition and/or unknown thermodynamic parameters.

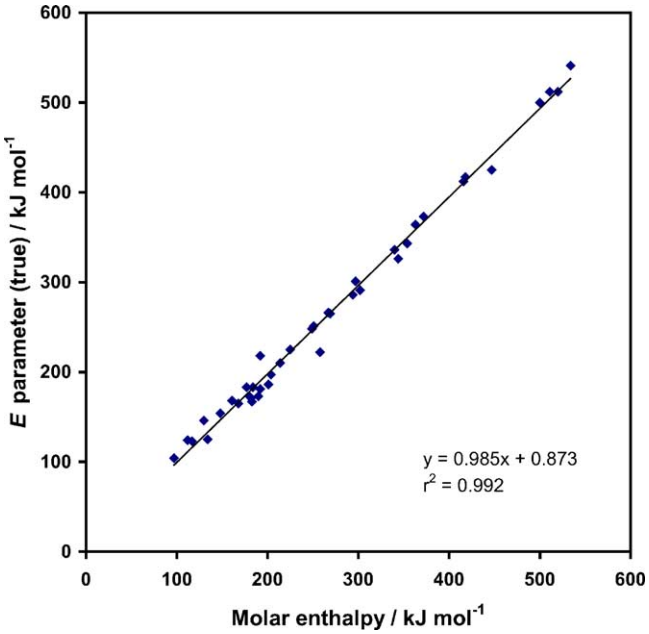

Fig. 5. Correlation between the molar enthalpies and the E parameters calculated by the precise version of the third-law method.

Table 8
Thermodynamic and kinetic parameters for thermal decompositions of reactants up to the solid and gaseous products

Deduced reaction[a]	ν	T (K)	$\Delta_{vap}H^{\circ}_T$ (kJ mol^{-1})	$-\Delta_c H^{\circ}_T$ (kJ mol^{-1})	τ[b]	$\Delta S^{\circ}_T/\nu$ (J mol^{-1} K^{-1})	P_{eq} (bar)	$\Delta_r H^{\circ}_T/\nu$ (kJ mol^{-1})	E (kJ mol^{-1})		Reference
									Third-law[c]	Reported	
$BN \rightarrow B(g)_{\downarrow} + 1/2N_2$	1.5	1800	808.2_{1800}	560.2_{1800}	0.012	154.7_{1800}	2.4×10^{-8}	534	541/507	329	[11]
$Pb(N_3)_2 \rightarrow Pb(g)_{\downarrow} + N + N_2 + N_3$	4	500	620.3_{300}	193.8_{500}	0.143	141.9_{300}	2.2×10^{-9}	148	154/151	125–159	[32]
$Pb_3O_4 \rightarrow 3PbO(g)_{\downarrow} + O$	4	730	1146.3_{700}	280.4_{700}	0.137	153.7_{700}	1.6×10^{-8}	258	222/226	188	[12]
$Be(OH)_2 \rightarrow BeO(g)_{\downarrow} + H_2O$	2	400	796.9_{400}	743.4_{400}	0.711	169.0_{400}	3.0×10^{-8}	134	125/122	115	[9]
$Mg(OH)_2 \rightarrow MgO(g)_{\downarrow} + H_2O$	2	535	710.4_{500}	632.2_{500}	0.614	163.9_{500}	1.5×10^{-8}	161	168/166	126–134	[9]
$Ca(OH)_2 \rightarrow CaO(g)_{\downarrow} + H_2O$	2	570	778.3_{600}	674.1_{600}	0.614	152.6_{600}	2.2×10^{-8}	182	171/175	145–174	[9]
$Sr(OH)_2 \rightarrow SrO(g)_{\downarrow} + H_2O$	2	590	706.6_{600}	579.3_{600}	0.558	151.3_{600}	7.8×10^{-9}	192	181/186	126	[9]
$Ba(OH)_2 \rightarrow BaO(g)_{\downarrow} + H_2O$	2	610	556.1_{600}	415.5_{600}	0.422	140.3_{600}	3.0×10^{-8}	190	173/185	63	[9]
$Zn(OH)_2 \rightarrow ZnO(g)_{\downarrow} + H_2O$	2	400	508.4_{300}	455.4_{300}	0.603	168.2_{300}	5.0×10^{-8}	117	123/120	95	[9]
$Cd(OH)_2 \rightarrow CdO(g)_{\downarrow} + H_2O$	2	385	400.8_{300}	340.1_{300}	0.522	164.4_{300}	5.0×10^{-9}	112	124/123	95–116	[9]
$AgNO_3 \rightarrow Ag(g)_{\downarrow} + NO_2 + 1/2O_2$	2.5	470	430.7_{470}	283.9_{500}	0.370	142.8_{470}	2.0×10^{-9}	130	146/142		[10]
$Cd(NO_3)_2 \rightarrow CdO(g)_{\downarrow} + 2NO_2 + O$	4	560	841.9_{600}	335.5_{600}	0.369	161.9_{600}	2.0×10^{-8}	180	174/172	177	[10]
$MgSO_4 \rightarrow MgO(g)_{\downarrow} + SO_2 + O$	3	1006	1262.6_{1000}	631.3_{1000}	0.387	171.3_{1000}	3.3×10^{-9}	340	336/324	312–343	[7]
$BaSO_4 \rightarrow BaO(g)_{\downarrow} + SO_2 + O$	3	1400	1237.3_{1400}	399.5_{1400}	−0.043	152.7_{1400}	2.7×10^{-8}	418	417/427	384	[7]
$MgCO_3 \rightarrow MgO(g)_{\downarrow} + CO_2$	2	670	728.1_{700}	630.9_{700}	0.544	174.3_{700}	1.4×10^{-8}	192	218/208	176	[5]
$1/2CaMg(CO_3)_2 \rightarrow 1/2CaO(g)_{\downarrow} + 1/2MgO(g)_{\downarrow} + CO_2$	2	810	815.3_{800}	650.9_{800}	0.488	164.5_{800}	3.9×10^{-8}	249	248/244	192	[3]
$CaCO_3 \rightarrow CaO(g)_{\downarrow} + CO_2$	2	910	840.6_{900}	669.4_{900}	0.454	157.3_{900}	1.0×10^{-7}	269	265/268	205	[2]
$SrCO_3 \rightarrow SrO(g)_{\downarrow} + CO_2$	2	910	805.6_{900}	566.9_{900}	0.383	161.1_{900}	1.0×10^{-8}	294	286/285	279	[5]
$BaCO_3 \rightarrow BaO(g)_{\downarrow} + CO_2$	2	1080	645.2_{1100}	406.0_{1100}	0.126	137.6_{1200}	4.5×10^{-8}	297	301/325	226	[5]
$Li_2SO_4 \cdot H_2O \rightarrow Li_2SO_4(g)_{\downarrow} + H_2O$	2	300	396.6_{298}	338.0_{298}	0.600	175.9_{298}	8.7×10^{-10}	97	104/100	51–87	[4,22]

[a] An arrow (↓) implies taking into account part τ of condensation energy consumed by the reactant.
[b] In calculation of $\Delta_r H^{\circ}_T/\nu$ values, the τ parameter was evaluated by Eq. (32).
[c] First value corresponds to $\Delta S^{\circ}_T/\nu$ listed in this table, and second value, to the average magnitude of $\Delta S^{\circ}_T/\nu$: 136 or 160 J mol^{-1} K^{-1} (see Section 3.2.3).

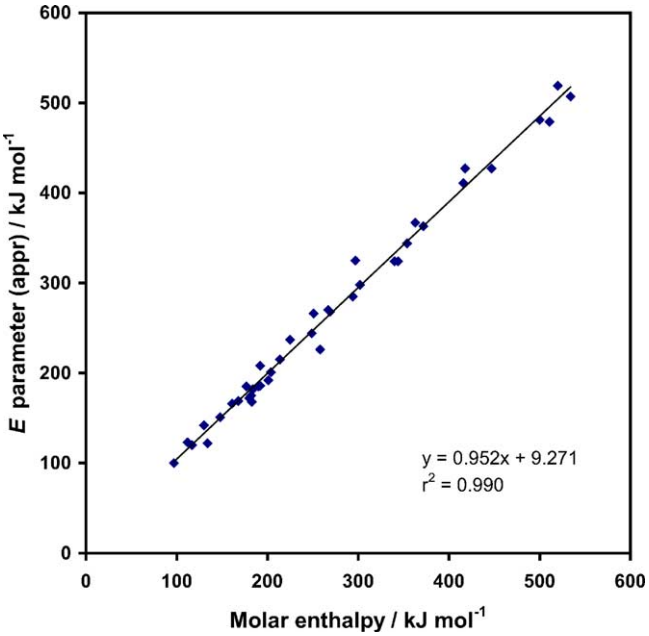

Fig. 6. Correlation between the molar enthalpies and the *E* parameters calculated by the approximate version of the third-law method.

4.6. Peculiarities in composition of primary gaseous products of decomposition

As can be seen from the analysis of data presented in Tables 7 and 8, the composition of primary gaseous products (oxygen, sulfur, selenium and nitrogen) in most cases differs from equilibrium. Wholly or in part, the evolution of these species proceeds in the form of free atoms. This problem is of profound theoretical and practical interest. By now, several general peculiarities were revealed in this field. The first of them is related to decomposition of Cd, Zn and Hg oxides [8]. These three oxides for IIB group of metals evaporate with formation of only gaseous products and, at first sight, the interpretation of the mechanism of their vaporization creates no problems. However, in fact, this is not the case. In contrast to the reversible dissociation of solid CdO up to Cd atoms and molecular oxygen (O_2), the decomposition of ZnO and HgO yields atomic oxygen (O). This was proved more than 40 years ago by Harano [34] by coloration in MoO_3 (from pale yellow to blue) in the process of ZnO, HgO, CuO and PtO_2 decomposition in vacuum. These mechanisms of evaporation were supported also by a good agreement of experimental values of the *E* parameters with theoretical values of the molar enthalpies for corresponding reactions and also, by results of investigation of the retardation effect of oxygen on the evaporation rate of ZnO, CdO and HgO [8].

The first attempt undertaken in [8] to explain this difference in mechanisms was to relate it to O–O distances in corresponding crystals. The minimum O–O distances for ZnO, CdO and HgO are as follows: 2.60, 3.34 and 3.50 Å. In all cases, these values are much higher than the internuclear distance in O_2 molecule (1.21 Å). However, this is not retarding the release of O_2 molecules in the process of CdO evaporation. It means that some other factors are responsible for the difference in mechanisms.

Table 9
Crystal structure and evaporation mechanism for some oxides and sulfates [8]

Oxide	Singony[a]	Space group	Minimum O–O distance (Å)	Primary product
Li_2O	I	225	2.31	O_2
Cu_2O	I	224	3.68; 4.25	O_2
Ag_2O	I	224	4.09; 4.72	O_2
MgO	I	225	2.98	O_2
CaO	I	225	3.39	O_2
SrO	I	225	3.63	O_2
CdO	I	225	3.34	O_2
MnO	I	225	3.14	O_2
FeO	I	225	3.06	O_2
CoO	I	225	3.01	O_2
NiO	I	225	2.95	O_2
PbO	II	129	1.98	O_2
CaO_2	II	139	4.62	O
SrO_2	II	139	3.55	O
BaO_2	II	139	5.12	O
GeO_2	II	136	2.86	O
SnO_2	II	136	3.19	O
Pb_3O_4	II	135	3.28	O
SiO_2	III	182	2.91	O
PtO_2	IIIa	164	2.74	O
ZnO	III	186	2.60	O
HgO	IV	62	3.50	O
$MgSO_4$	IV	63	2.47	O
$BaSO_4$	IV	62	2.44	O
CuO	V	15	2.62	O

[a] I: cubic; II: tetragonal; III: hexagonal; IIIa: trigonal; IV: rhombic; V: monoclinic.

To investigate the situation in more detail, L'vov et al. [8] collected all available data on the evaporation mechanisms of 23 different oxides (and two sulfates) and correlated them with their crystal structure (Table 9). When all these compounds were arranged into two groups differed in the releasing mechanism of oxygen, some remarkable differences in their crystal structure have been appeared. As can be seen from these data, all oxides, which evaporate with the release of molecular oxygen, except for PbO, are of the cubic singony (I). For all other compounds of different (from cubic) singony (II, III, IIIa, IV or V), the release of oxygen occurs in the form of free O atoms. As for PbO, the release of molecular oxygen can be connected with the anomalously small O–O distance (1.98 Å) in comparison with those for other oxides.

The author is not ready now to propose any quantitative explanation of this phenomenon. The only obvious conclusion consists in correlation of these differences with the structure symmetry. It can be proposed that a decisive role here belongs to a local symmetry in the position of O atoms. For those oxides, where this symmetry is the highest and environment is close to isotropic, there is the molecular mechanism of dissociation. Oxygen atoms, which are in

Table 10
Decomposition mechanism of nitrides vs. their crystal structure [11]

Deduced reaction	Singony[a]	Space group	Minimum N–N distance (Å)
c-BN → $B(g)_{\downarrow}$ + 1/2N_2	I	216	2.56
c-AlN → Al(g) + 1/2N_2	I	216	3.09
c-GaN → Ga(g) + 1/2N_2	I	216	3.09
Be_3N_2 → 3Be(g) + N + 1/2N_2	III	194	2.84
Mg_3N_2 → 3Mg(g) + N + 1/2N_2	I	206	3.29
h-BN → B(g) + 1/2N + 1/4N_2	IIIa	164	2.51
h-AlN → Al(g) + 1/2N + 1/4N_2	III	186	3.07
h-GaN → Ga(g) + 1/2N + 1/4N_2	III	186	3.17
InN → In(g) + 1/2N + 1/4N_2	III	186	3.51
α,β-Si_3N_4 → 3Si(g) + 2N + N_2	III	159; 176	2.82; 2.79

[a] I: cubic; III: hexagonal; IIIa: trigonal.

low-symmetrical positions, release their sites without recombination. It is probable that there are some differences in electronic structure of these atoms responsible for the mechanism of recombination. These conclusions deserve further investigation and application to decomposition studies for other compounds.

The other interesting phenomenon revealed from consideration of the data presented in Table 7 is the decomposition of metal selenides and sulfides (CdSe, ZnSe and ZnS) and nitrides (AlN, GaN, InN, Be_3N_2, Mg_3N_2 and Si_3N_4) with evolution of primary atomic (Se, S and N) and molecular (Se_2, S_2 and N_2) species in the molar quantities related as 2–1. However, there are some exceptions. As can be seen from Table 10, in which decomposition reactions for all nitrides are correlated with their crystal structure, nitrides with the cubic (I) singony (except of Mg_3N_2) decompose, as in the case of oxides, with the release of only molecular nitrogen. These peculiarities undoubtedly deserve further study.

4.7. Interpretation of coefficient of decomposition

By the coefficient of decomposition (or vaporization in the case of the sublimation of simple substances), α, one usually refers the ratio of the real gaseous-product flux, J, to the flux, J_{max}, from the effusion cell wherein the decomposition products are expected to attain their ideal equilibrium partial pressures. Judging from numerous experimental measurements, $\alpha \ll 1$ for many substances, i.e., they decompose more slowly than expected based on effusion-cell experiments. This discrepancy is usually attributed to the multi-stage character of the evaporation process, specific features of surface relief and impurities and lattice defects of the reactant [35].

L'vov and Novichikhin [31] pioneered in explanation of this effect as due to the difference between the true scheme of thermal decomposition of a given compound and one which assumes direct decomposition to the final products in thermodynamic equilibrium (as is the case in the effusion cell). These differences consist, first, in primary gasification of all decomposition products, including low-volatility components (metals and metal oxides) and, second, in the partial or total evolution of gaseous species in a form different from the equilibrium composition (Section 4.6).

To illustrate the impact of these factors on the decomposition coefficient, we present in Tables 11 and 12 the corresponding data for some hydroxides and azides. In case of hydroxides (Table 11), only the first factor is responsible for low values of decomposition coefficient. In case of NaN_3 and KN_3 (Table 12), the second factor determines the α values. Finally, in case of $Pb(N_3)_2$ both factors are important. As a result of this 'double distinction' in the overall composition of primary products, the decomposition coefficient is much lower than in other cases. Some of these compounds with very low decomposition coefficients (azides and oxalates) are explosives. Nevertheless, because they decompose into primary products very different from equilibrium products, they are rather stable at room temperature.

Table 11
Coefficients of decomposition for some hydroxides at the initial decomposition temperatures[a]

Hydroxide	T (K)	Primary products	P_{eq} [9] (bar)	Equilibrium products	P_{id} (bar)	α
$Ba(OH)_2$	600	$BaO(g)_{\downarrow}$ + H_2O	3.0×10^{-8}	BaO(s) + H_2O	4.1×10^{-6}	7×10^{-3}
$Sr(OH)_2$	592	$SrO(g)_{\downarrow}$ + H_2O	8.0×10^{-9}	SrO(s) + H_2O	9.9×10^{-5}	8×10^{-5}
$Ca(OH)_2$	600	$CaO(g)_{\downarrow}$ + H_2O	5.7×10^{-8}	CaO(s) + H_2O	7.6×10^{-3}	8×10^{-6}
$Mg(OH)_2$	510	$MgO(g)_{\downarrow}$ + H_2O	5.8×10^{-9}	MgO(s) + H_2O	4.7×10^{-1}	1×10^{-8}
$Be(OH)_2$	396	$BeO(g)_{\downarrow}$ + H_2O	2.9×10^{-8}	BeO(s) + H_2O	9.7	3×10^{-9}
$Zn(OH)_2$	390	$ZnO(g)_{\downarrow}$ + H_2O	3.0×10^{-8}	ZnO(s) + H_2O	10.3	3×10^{-9}
$Cd(OH)_2$	385	$CdO(g)_{\downarrow}$ + H_2O	5.0×10^{-9}	CdO(s) + H_2O	3.3×10^{11}	2×10^{-20}

[a] P_{eq} and P_{id} are, respectively, the real equivalent and ideal equilibrium pressures of gaseous products measured in the former case and calculated in the latter.

Table 12
Coefficients of decomposition for some azides at the initial decomposition temperatures[a]

Azide	T (K)	Primary products	P_{eq} [32] (bar)	Equilibrium products	P_{id} (bar)	α
NaN_3	603	$Na(g) + N_2 + N$	3.4×10^{-8}	$Na(g) + 1.5N_2$	1.6×10^{4}	2×10^{-11}
KN_3	524	$K(g) + N_2 + N$	7.3×10^{-9}	$K(g) + 1.5N_2$	0.94	8×10^{-9}
$Pb(N_3)_2$	500	$Pb(g)_{\downarrow} + N + N_2 + N_3$	2.2×10^{-9}	$Pb(s) + 3N_2$	8.2×10^{24}	3×10^{-34}

[a] P_{eq} and P_{id} are, respectively, the real equivalent and ideal equilibrium pressures of gaseous products measured in the former case and calculated in the latter.

The low magnitudes of decomposition coefficient ($<10^{-10}$ and even $<10^{-30}$) are in contrary with the widespread statement (opinion) that α value varies for different reactants in the range from 1 to 10^{-6} [35]. This delusion is connected with limitations of the effusion (Knudsen cell) method, which used for evaluation of the maximum decomposition rate or true equilibrium pressure of products. Indeed, the ratio of equilibrium pressure inside a cell to pressure of effusing gas is described by equation [36]:

$$\frac{P_0}{P_m} \cong 1 + \frac{sW_C}{S\alpha} \tag{35}$$

where s and S are the orifice area and evaporating surface area, respectively (the cross-section of the cell) and W_C the Clausing factor. To measure P_m value with the error lower than 10% it is necessary to satisfy the condition $P_0/P_m \leq 1.1$ or

$$\alpha \geq 10\frac{sW_C}{S} \tag{36}$$

Taking into account that W_C is in the range 0.2–0.8 and $s/S > 10^{-5}$ [36], we can conclude that α should be higher than 10^{-5} to satisfy the condition of more or less correct measurement of true equilibrium pressure. Otherwise, the pressure inside a cell does not reach the equilibrium.

4.8. Evaluation of the self-cooling effect

The significance of the self-cooling effect in the process of endothermic decomposition reactions has been discussed in many works on thermal analysis. However, only a few studies [37,38] performed in the period of 1930–1950 are known, which take into account this effect in measurements of the dehydration rates and the corresponding Arrhenius parameters (E and A). Most other workers assume (in many cases, tacitly) that the value of self-cooling is negligible and might have been ignored in such measurements. (Much more interest has been expressed in the problem of self-heating during pyrolysis, carbon gasification and decomposition of energetic materials. As an example, the isoconversional method has been developed recently for kinetic studies of materials when a reaction system undergoes arbitrary variation of the temperature [39].)

In 1998, L'vov et al. published a series of papers [15,16,22] devoted to the quantitative modeling of temperature distribution in heterogeneous systems and evaluation of the effect of self-cooling on the decomposition parameters of $Mg(OH)_2$ and $Li_2SO_4{\cdot}H_2O$ (see Section 3.2.2). It was shown that the temperature difference between the temperature controlled heater and the sample (even for a single crystal) can reach in high vacuum under other typical conditions several ten degrees and introduce serious errors in the determination of kinetic parameters. Despite this justified warning, the situation has not been improved.

Unfortunately, any simple and reliable techniques for experimental determination of self-cooling in TA are absent. (The use of a thermocouple junction inserted between two cemented together large crystals applied by Cooper and Garner [37] and Anous et al. [38] for measuring the real temperature of the chrome alum crystals is the sole exception). This hindered the verification of the above theoretical conclusion. The situation has been changed only recently after appearance in TA of the third-law methodology [1].

The magnitude of the self-cooling can be easily estimated from Eqs. (15) and (16) if we assume that the only reason of overestimation for the experimental E_{exp} value, calculated by the third-law method, is the effect of self-cooling. If we further assume that the E value at the lowest measurement temperature is free from this effect (i.e., the temperature of the sample, T_s, is equal to the temperature of the heater, T_h) and corresponds to the true value of the E parameter, E_{true}, then it is possible to find the actual temperature of the sample, T_s, for any higher temperature of decomposition. This temperature is equal:

$$T_s = T_h\frac{E_{true}}{E_{exp}} \tag{37}$$

if we neglect a small systematic decrease of both $\Delta_r S^\circ_T$ and $\Delta_r H^\circ_T$ values with temperature.

This simple technique was successfully used in [2–5]. Table 13 presents some of the data received in these works for several carbonates and hydrates. As can be seen, in full accord with the above theoretical (model) evaluations, the temperature difference between the temperature controlled heater and the sample in high vacuum constitutes several ten degrees and can reach (in extreme cases) about 10% of the heater temperature. This systematic error manifests in significant (15–30%) underestimation of the E parameters in many cases of application of the second-law and Arrhenius-plots methods. It is remarkable that this effect is most conspicuous for reactants decomposed with formation of solid products (see Table 8). As can be seen from the

Table 13
Effect of self-cooling in the process of decomposition of some solids in vacuum evaluated by the third-law method [2–5]

Reactant	T_{max} (K)	Sample	P_{eq} (bar)	ΔT at T_{max} (K)
$CaCO_3$	1013	Crystal	5×10^{-7}	−90
	948	Crystal	1×10^{-7}	−66
$CaMg(CO_3)_2$	900	Crystal	4×10^{-7}	−49
$BaCO_3$	1232	Powder	6×10^{-7}	−54
$Li_2SO_4 \cdot H_2O$	433	Crystal	1×10^{-5}	−43
	400	Crystal	7×10^{-6}	−27
	363	Crystal	7×10^{-8}	−18
$CaSO_4 \cdot 2H_2O$	357	Crystal	4×10^{-7}	−11
$CuSO_4 \cdot 5H_2O$	303	Crystal	8×10^{-8}	−6

results of decomposition of reactants up to the gaseous products (Table 7), only for 3 of the 20 reactants (SnO_2, GaN and Mg_3N_2), the results of determination of the E parameters by the second-law and Arrhenius-plots methods are lower than those measured by the third-law method.

This difference is easy to explain [2]. In case of formation of solid product on the surface of reactant, heating of reactant in high vacuum by radiation from the heater (for example, from the wall of alumina crucible) occurs through the intermediate layer of this product (e.g., CaO in case of decomposition of $CaCO_3$). It means that the effective value of the emittance factor corresponding to the heat radiation transfer from the alumina crucible to the calcite crystal covered by a layer of CaO product is actually a product of the emittance factors for all four surfaces: Al_2O_3, CaO (external), CaO (internal) and $CaCO_3$. (We neglect here the residual heat conduction via point contacts between a $CaCO_3$ reactant and nano-crystals of CaO product.) If we take into account that at 900 K the emittance factor, ε, for each of these surfaces is about 0.3 [14], than the product of these four factors, ε^*, is equal to about 0.01. This value is very close to the magnitude ($\varepsilon^* = 0.015$) successfully used by L'vov [40] for theoretical modeling of the Topley–Smith effect in case of the decomposition of calcite in the presence of CO_2 and is very far from that ($\varepsilon^* = 0.3$–0.5) assumed by Powell and Searcy [41] in their modeling of "the heat balance during steady state decomposition of $CaCO_3$ single crystals in vacuum". This is a key reason of disagreement between our [1–5,40] and Searcy and coworkers [41,42] opinions on the problem of self-cooling under high-vacuum conditions.

We should repeat again a conclusion made in [1,40]: the belief expressed by Powell and Searcy [41] (contrary to the contention of others, the rate of decomposition of $CaCO_3$ can be measured under conditions, which make the slowest chemical step of the process, rather than heat transfer or gas phase diffusion, rate limiting) and by Beruto and Searcy [42] (the design of the apparatus used in the present study reduces the heat transfer problem to a negligible source of error in the temperature and decomposition pressure range used) was too optimistic. Only in the absence of solid product on the surface of reactant, when the effective value $\varepsilon^* > 0.1$, the effect of self-cooling can be neglected.

5. Conclusions

The most important results obtained since the first application (in 2002) of the third-law methodology to kinetic studies of decomposition reactions can be formulated as follows:

1. The method has been significantly improved and extended to powdered and melted materials. The use of the average values of molar entropy greatly simplified its application to materials with unknown product composition and/or unknown thermodynamic parameters. The order of magnitude higher precision and low susceptibility of the third-law method to the self-cooling compared with the Arrhenius-plots method, guarantees measurement of the E parameter with the error less than 2%. A significant reduction of experimental time and a possibility of simple evaluation of self-cooling are the additional advantages of this method.
2. The application of the third-law method to decomposition studies permitted to support the basic assumptions underlying PA-theory. A good fit of experiment to theory for the ratio of the initial decomposition temperature to the E parameter, the peculiarities of carbonate decomposition in CO_2 and regularities of solid and melted nitrate decomposition are in complete agreement with the mechanism of dissociative evaporation and consumption of a part τ of the condensation energy by the reactant. No other quantitative explanations for these regularities could be proposed. It has become possible to evaluate the τ parameter a priori on the basis of thermodynamic features of the low-volatility product. As a consequence, the physical approach gains the features of completed self-consistent theory. From comparison of the E parameters with the molar enthalpies of the implied reactions, the decomposition mechanisms of a large group of reactants from different classes of chemical compounds are identified on a single basis. Some peculiarities in evolution of gaseous products in atomic and molecular forms are interpreted in accordance with the crystal symmetry of reactants. Last but not least, earlier theoretical estimations of the self-cooling effect, which can reach in high vacuum several ten degrees, are supported experimentally.

It is difficult to imagine how much effort, time and money have been spent in vain in the investigations of kinetics of solid decompositions because of neglecting the third-law method. Why not try it now!

Acknowledgements

The author thanks Dr. Valery Ugolkov (Institute of Silicate Chemistry, St. Petersburg) who carried out most of experimental work over the last 3 years, as well as other colleagues (Dr. L.K. Polzik, Prof. F.F. Grekov and assistants

A.V. Novichikhin and A.O. Dyakov) who participated in separate stages of this study. The author is also grateful to Dr. A.K. Galwey (Belfast) for a continual moral support of these investigations.

References

[1] B.V. L'vov, The interrelation between the temperature of solid decompositions and the *E* parameter of the Arrhenius equation, Thermochim. Acta 389 (2002) 199–211.
[2] B.V. L'vov, L.K. Polzik, V.L. Ugolkov, Decomposition kinetics of calcite: a new approach to the old problem, Thermochim. Acta 390 (2002) 5–19.
[3] B.V. L'vov, V.L. Ugolkov, Kinetics of free-surface decomposition of dolomite single crystals and powders analyzed thermogravimetrically by the third-law method, Thermochim. Acta 401 (2003) 139–147.
[4] B.V. L'vov, V.L. Ugolkov, The self-cooling effect in the process of dehydration of $Li_2SO_4{\cdot}H_2O$, $CaSO_4{\cdot}2H_2O$ and $CuSO_4{\cdot}5H_2O$ in vacuum, J. Therm. Anal. Calorim. 74 (2003) 697–708.
[5] B.V. L'vov, V.L. Ugolkov, Kinetics of free-surface decomposition of magnesium, magnesium, strontium and barium carbonates analyzed thermogravimetrically by the third-law method, Thermochim. Acta 409 (2004) 13–18.
[6] B.V. L'vov, V.L. Ugolkov, Peculiarities of $CaCO_3$, $SrCO_3$ and $BaCO_3$ decomposition in CO_2 as a proof of their primary dissociative evaporation, Thermochim. Acta 410 (2004) 47–55.
[7] B.V. L'vov, V.L. Ugolkov, Kinetics of free-surface decomposition of magnesium and barium sulfates analyzed thermogravimetrically by the third-law method, Thermochim. Acta 411 (2004) 73–79.
[8] B.V. L'vov, V.L. Ugolkov, F.F. Grekov, Kinetics of free-surface evaporation of zinc, cadmium and mercuric oxides analyzed thermogravimetrically by the third-law method, Thermochim. Acta 411 (2004) 187–193.
[9] B.V. L'vov, V.L. Ugolkov, Kinetics of free-surface decomposition of group IIA and IIB hydroxides analyzed thermogravimetrically by the third-law method, Thermochim. Acta 413 (2004) 7–15.
[10] B.V. L'vov, V.L. Ugolkov, Kinetics and mechanism of free-surface decomposition of solid and melted $AgNO_3$ and $Cd(NO_3)_2$ analyzed thermogravimetrically by the third-law method, Thermochim. Acta 2004 (424) 7–13.
[11] B.V. L'vov, V.L. Ugolkov, Kinetics and mechanism of free-surface vaporization of group IIA, IIIA and IVA nitrides analyzed thermogravimetrically by the third-law method, Thermochim. Acta, in preparation.
[12] B.V. L'vov, V.L. Ugolkov, Kinetics and mechanism of free-surface decomposition of Pb_3O_4 analyzed thermogravimetrically by the third-law method, J. Therm. Anal. Calorim., in press.
[13] B.V. L'vov, Interpretation of atomization mechanisms in electrothermal atomic absorption spectrometry by analysis of the absolute rates of the processes (review), Spectrochim. Acta B 52 (1997) 1–23.
[14] I.K. Kikoin, Tables of Physical Constants, Atomizdat, Moscow, 1976 (in Russian).
[15] B.V. L'vov, A.V. Novichikhin, A.O. Dyakov, Mechanism of thermal decomposition of magnesium hydroxide, Thermochim. Acta 315 (1998) 135–143.
[16] B.V. L'vov, A.V. Novichikhin, A.O. Dyakov, Computer simulation of the Topley–Smith effect, Thermochim. Acta 315 (1998) 169–179.
[17] V.P. Glushko (Ed.), Thermodynamic Properties of Individual Substances, Handbook, vols. 1–4, Nauka, Moscow, 1978–1982 (in Russian).
[18] V.P. Glushko (Ed.), Thermodynamic Constants of Substances, Handbook, vols. 1–10, Akad. Nauk SSSR, Moscow, 1965–1982 (in Russian).
[19] V.A. Kireev, Methods of Practical Calculations in Thermodynamics of Chemical Reactions, Khimiya, Moscow, 1975 (in Russian).
[20] V.A. Ryabin, M.A. Ostroumov, T.F. Svit, Thermodynamic Characteristics of Substances, Handbook, Khimiya, Leningrad, 1977 (in Russian).
[21] D.T. Beruto, R. Vecchiattini, M. Giordani, Solid products and rate-limiting step in the thermal half decomposition of natural dolomite in a CO_2(g) atmosphere, Thermochim. Acta 405 (2003) 183–194.
[22] B.V. L'vov, Mechanism of thermal decomposition of $Li_2SO_4{\cdot}H_2O$, Thermochim. Acta 315 (1998) 145–157.
[23] B.V. L'vov, Kinetics and mechanism of thermal decomposition of nickel, manganese, silver, mercury and lead oxalates, Thermochim. Acta 364 (2000) 99–109.
[24] A.K. Galwey, Thermal reactions of selected solids including reactants that melt during chemical change, J. Therm. Anal. 41 (1994) 267–286.
[25] A.K. Galwey, M.E. Brown, Thermal Decomposition of Ionic Solids, Elsevier, Amsterdam, 1999, p. 203.
[26] B.V. L'vov, A.V. Novichikhin, Mechanism of thermal decomposition of anhydrous metal nitrates, Spectrochim. Acta B 50 (1995) 1427–1448.
[27] C. Ettarh, A.K. Galwey, A kinetic and mechanistic study of the thermal decomposition of calcium nitrates, Thermochim. Acta 288 (1996) 203–219.
[28] B.V. L'vov, G.N. Ryabchuk, Studies of the mechanisms of sample atomization in electrothermal atomic absorption spectrometry by analysis of absolute process rates. Oxygen-containing compounds, Zh. Anal. Khim. 36 (1981) 2085–2096 (in Russian).
[29] S. Vyazovkin, Thermal analysis (review), Anal. Chem. 74 (2002) 2749–2762.
[30] G.N. Lewis, Zersetzung von Zilberoxyd durch Autokatalyse, Z. Phys. Chem. 52 (1905) 310–326.
[31] B.V. L'vov, A.V. Novichikhin, Quantitative interpretation of the evaporation coefficients for the decomposition or sublimation of some substances in vacuo, Thermochim. Acta 290 (1997) 239–251.
[32] B.V. L'vov, Mechanism of thermal decomposition of metal azides, Thermochim. Acta 291 (1997) 179–185.
[33] B.V. L'vov, Unpublished data.
[34] Y. Harano, The detection of atomic oxygen in the decomposition of some metallic oxides, Nippon Kagaku Zasshi 82 (1961) 152–155 (in Japanese).
[35] J.F. Dettorre, T.G. Knorr, E.H. Hall, Evaporation processes, in: C.F. Powel, J.H. Oxley, J.M. Blocher Jr. (Eds.), Vapor Deposition, Wiley, New York, 1966, pp. 62–101.
[36] A.N. Nesmeyanov, Vapor Pressure of Chemical Elements, Akad. Nauk SSSR, Moscow, 1961, pp. 38–44 (in Russian).
[37] M.M. Cooper, W.E. Garner, The dehydration of crystals of chrome alum, Proc. Roy. Soc. A 174 (1940) 487–503.
[38] M.M. Anous, R.S. Bradley, J. Colvin, The rate of dehydration of chrome alum, J. Chem. Soc. (1951) 3348–3354.
[39] S. Vyazovkin, Evaluation of activated energy of thermally stimulated solid-state reactions under arbitrary variation of temperature, J. Comp. Chem. 18 (1997) 393–402.
[40] B.V. L'vov, Mechanism and kinetics of thermal decomposition of carbonates (review), Thermochim. Acta 386 (2002) 1–16.
[41] E.K. Powell, A.W. Searcy, The rate and activation enthalpy of decomposition of $CaCO_3$, Met. Trans. B 11 (1980) 427–432.
[42] D. Beruto, A.W. Searcy, Use of the Langmuir method for kinetic studies of decomposition reactions: calcite ($CaCO_3$), J. Chem. Soc. Faraday Trans. I 70 (1974) 2145–2153.